Neuroserpin polymers activate NF-kappaB by a calcium signaling pathway that is independent of the unfolded protein response.

Mark J Davies, Elena Miranda, Benoit D Roussel, Randal J Kaufman, Stefan J Marciniak, David A Lomas

Neuroserpin polymers activate NF-κB by a calcium signalling pathway that is independent of the unfolded protein response

Mark J. Davies[1], Elena Miranda[1], Benoit D. Roussel[1], Randal J. Kaufman[2], Stefan J. Marciniak[1*] and David A. Lomas[1*§]

[1]Department of Medicine, University of Cambridge, Cambridge Institute for Medical Research, Wellcome Trust/MRC Building, Hills Road, Cambridge. CB2 0XY, UK. [2]Departments of Biological Chemistry and Internal Medicine and the HHMI, University of Michigan Medical Center, Ann Arbor MI 48109, USA.

* Joint senior authors

§To whom correspondence should be addressed: E-mail: dal16@cam.ac.uk
Telephone: (+44) 1223 762818
Fax: (+44) 1223 336827

Short Title: Neuroserpin polymers and the ER overload response

Key Words: ER stress, UPR, EOR, serpin, serpinopathies, conformational diseases

Summary

The autosomal dominant dementia familial encephalopathy with neuroserpin inclusion bodies (FENIB) is characterized by the accumulation of ordered polymers of mutant neuroserpin within the endoplasmic reticulum of neurones. We show here that intracellular neuroserpin polymers activate NF-κB by a pathway that is independent of the IRE1, ATF6 and PERK limbs of the canonical unfolded protein response, but is dependent on intracellular calcium. This pathway provides a mechanism for cells to sense and react to the accumulation of folded structures of mutant serpins within the endoplasmic reticulum. Our results provide strong support for the endoplasmic reticulum overload response being independent of the unfolded protein response.

Introduction

An increasing number of disorders are recognised to result from the aggregation and tissue deposition of misfolded proteins. Indeed, their shared mechanism provides the basis for a new class of disorder, the conformational diseases (1). These include Alzheimer's, Huntington's and Parkinson's diseases as well as the amyloidoses and serpinopathies. The serpinopathies are characterized by the aggregation and tissue deposition of members of the serine protease inhibitor or serpin superfamily of proteins (2). Point mutations of serpins such as α_1-antitrypsin, antithrombin and α_1-antichymotrypsin result in a sequential linkage between the exposed mobile reactive centre loop of one molecule and β-sheet A of another (3,4). The resulting ordered polymers then accumulate as inclusion bodies within the lumen of the endoplasmic reticulum (ER) (1,2). This is associated with disease due to loss of function (i.e. the reduction in active protein) and/or a toxic gain of function (i.e. the cytotoxicity of protein aggregates).

One of the most striking serpinopathies is the autosomal dominant dementia familial encephalopathy with neuroserpin inclusion bodies or FENIB (5). This results from one of four naturally occurring point mutations in the neuroserpin gene: S49P, S52R, H338R or G392E

(6). The mutant neuroserpin proteins form ordered polymers that accumulate in the ER of neurones within the cerebral cortex, hippocampus and substantia nigra (5-7). The resulting inclusions lead to progressive dementia, with the age of onset of disease being inversely proportional to the rate at which the mutants form polymers *in vitro* and the number of intra-cerebral inclusions (6).

The accumulation of misfolded proteins within the lumen of the ER activates the PERK (PKR-like endoplasmic reticulum kinase), IRE1 (inositol requiring kinase 1) and ATF6 (activating transciption factor 6) limbs of the unfolded protein response (UPR). This pathway serves to attenuate protein translation and increase the production of molecular chaperones to promote polypeptide folding and remove terminally misfolded proteins by ER associated degradation (ERAD) (8). The UPR is increasingly being implicated in the pathogenesis of human disease (9). It is striking that accumulation of mutant Z α_1-antitrypsin polymers within the ER of hepatocytes does not elicit the UPR (10) but does activate NF-κB (11,12). This has been explained by the activation of the ER overload response (EOR) (13), a stress signalling pathway that links the accumulation of folded proteins within the ER with the activation of NF-κB. The term EOR was originally coined to describe the NF-κB response to ER accumulation of viral proteins (14), but was subsequently extended to include other proteins retained within the ER despite achieving native or near native conformations (15,16). However, NF-κB activation in response to ER dysfunction has been shown to require PERK signalling and so the very existence of an EOR pathway distinct from the UPR remains controversial (17).

Here we have used wildtype and mutants of neuroserpin to investigate the consequences of ordered protein accumulation within the ER. We demonstrate that neuroserpin polymers activate NF-κB by a calcium dependent pathway that is independent of the IRE, ATF6 and PERK limbs of the canonical UPR. These data provide strong support for a signalling pathway that directly links the activation of NF-κB with the accumulation of ordered proteins within the ER.

Experimental procedures

Antibodies and reagents. The rabbit polyclonal anti-neuroserpin antibody was produced by Abcam (Cambridge, UK) using purified recombinant wild type neuroserpin as the antigen (18). Rabbit polyclonal anti-GAPDH and donkey polyclonal anti-rabbit IgG (Texas Red) antibodies were also from Abcam. Goat polyclonal anti-rabbit IgG (HRP) and rabbit polyclonal anti-mouse IgG (HRP) antibodies were from Sigma-Aldrich Co (Dorset, UK). Rabbit polyclonal anti-Phospho-eIF2α (S51) from Cell Signaling was a kind gift from Dr Shiu-Wan Chan (Faculty of Life Sciences, University of Manchester, UK). All pharmacological cell-permeable inhibitors were purchased from Calbiochem (Merck Chemicals Ltd, Nottingham, UK). Unless stated otherwise, reagents for cell culture were purchased from Sigma-Aldrich Co (Dorset, UK).

Culture of stable PC12 Tet-On cells lines expressing neuroserpin. The cells were cultured in DMEM supplemented with 10% v/v heat inactivated horse serum, 5% v/v Tet Approved FBS (BD Biosciences), 10 mM HEPES, 1× non-essential amino acids, 0.2 U/ml bovine insulin, 200 μg/ml Geneticin and 100 μg/ml Hygromycin B (selective antibiotics from Invitrogen, Paisley, UK), and incubated at 37 $^{\circ}$C and 5% v/v CO_2 in a humidified incubator. Neuroserpin expression was typically induced with 10 μg/ml doxycycline (BD Biosciences).

Mouse Embryonic Fibroblast (MEF) eIF2α-S51A Cell Line. Immortalised wild type and eIF2α $S51^{A/A}$ MEFs were transduced with pBABE retrovirus encoding WT, S52R, G392E and ΔNS neuroserpin using previously described protocols (19,20). Briefly, cells were selected for stable transgene expression by selection with 2.5 μg/ml puromycin, with surviving cells considered as stable expressing pools. Several stable pools expressing neuroserpin were established and these were then used in the functional studies. All results described are the average of at least three independent repeats.

SDS and non-denaturing PAGE and Western Blot analysis. Cell lysates and culture media were analysed in 10% w/v SDS PAGE or 7.5% w/v

acrylamide non-denaturing gels as described previously (21).

Metabolic labelling and immunoprecipitation. Metabolic labelling experiments with ^{35}S-met/cys were performed as described previously (21). PC12 cells were treated with 200 μM leupeptin, 25 μM lactacystin or 3 μM brefeldin A from Calbiochem (CN Biosciences, Nottingham, UK) for 1 hr prior to starvation and these agents were present in all subsequent steps until harvesting.

RT-PCR and XBP1 *Splicing Assay.* Total RNA was isolated from mammalian cells using the recommended protocol in the Qiagen RNeasy Isolation kit. (Qiagen, UK). The concentration of RNA was determined and 1 μg of total RNA was used as a template for first strand cDNA synthesis using the manufactures recommended protocols (Promega UK Ltd.). This was then used to semi-quantify the relative levels of neuroserpin and β-actin mRNA expression, and also the unspliced to spliced ratio of XBP1. The primers were RT_NS_S (5'-TCT CCA TTG AGT ATT GCT CTT GC), RT_NS_AS (5'-TCT CCT TGC TGA TAC ATC ATT GG), Actin_S (5'-CTT CGC GGG CGA CGA TGC), Actin_AS (5'-TGG TGG TGA AGC TGT AGC C), RtXBP1S (5'- AAA CAG AGT AGC AGC ACA GAC TGC) and RtXBP1AS (5'- TCC TTG TGG GTA GAC CTC TGG GAG). Optimal PCR conditions were used as described previously (22).

Luciferase Assay. Transfections were performed in 6-well plates that had been pre-coated with 0.1 mg/ml poly-L-lysine. Typically, 2 μg of either p(5×)ATF6-luc (firefly) or pELAM1-luc (firefly) and 50 ng of pRL-TK (renilla) transfection efficiency control reporter plasmids (all kind gifts from Dr. Timothy Weaver, Cincinnati Children's Hospital Medical Center, Ohio, USA) were mixed with 6.25 μl of Lipofectamine 2000 (Invitrogen, Paisley, UK) in serum free Opti-MEM culture medium (GIBCO, Invitrogen, UK) following the manufactures protocol. The cells were lysed post-transfection using the Dual-Luciferase Reporter Assay (Promega, UK) recommended protocol in 1× passive lysis buffer. Both firefly and renilla luciferase activity were measured using a Glomax Luminometer (Promega, UK), and firely luciferase activity was calculated relative to renilla transfection efficiency. All measurements were performed in triplicate.

Ca^{2+} Flux Measurements. PC12 cells were resuspended at a concentration of 1×10^6 cells/ml and loaded with Fluo-4 NW dye assay buffer (Invitrogen, Paisley, UK) according to the manufactures recommend protocol for 30 min at 37 °C and then 15 min at room temperature. The cells were then loaded onto a FACS Calibur cell cytometer (BD Biosciences, Oxford, UK) and read at 488 nm over time. Calcium was mobilised by the addition of 1 μM thapsigargin (TG) and the measurements continued to a relative increase in fluorescence that was stable over time. Control cells were pre-treated with 2 μg/ml tunicamycin for 16 hr or the calcium store was depleted by the addition of 1 μM TG for 30 min and recovery for 1 hr in fresh media before analysis. All experiments were performed in triplicate and analysed with FlowJo software (BD Biosciences, Oxford, UK).

Statistical analysis. When comparing within a series, for example when analysing the effects of a drug on each cell line, paired t-test was used. When comparing data between series 2-way ANOVA with a Bonferroni post test was used.

Results

Mutants of neuroserpin accumulate within the endoplasmic reticulum of PC12 cells

In order to study the cellular responses to the expression of mutant neuroserpin, we used rat pheochromocytoma (PC12) Tet-On cell lines that conditionally expressed wildtype human neuroserpin (WT) or the S52R and G392E mutants that are associated with moderate and severe forms of the dementia FENIB respectively ((23) and Fig. 1a). In addition, we generated a stable cell line that expressed a novel misfolding mutant of neuroserpin, with deletion of the C-terminal 134 amino acids, which include the reactive loop (ΔNS) (Fig. 1a). This mutant is equivalent to the null Hong Kong variant of the serpin α_1-antitrypsin, which cannot form ordered polymers

and is an efficient activator of the UPR and a potent substrate for ERAD (24). We first assessed the presence of neuroserpin in these cells lines by SDS-PAGE and Western Blot analysis (Supplementary Fig. 1). All four PC12 cell lines expressed neuroserpin when the cells were treated with increasing concentrations of doxycycline. WT, S52R and G392E neuroserpin migrated with a molecular mass of 50 kDa, while the truncated version of neuroserpin, ΔNS, migrated at 28 kDa. Our previous work showed that in these cell lines WT neuroserpin was mainly stored in secretory granules at the tips of neurites, characteristic of a protein secreted through the regulated secretory pathway (23). In contrast, S52R and G392E neuroserpin formed inclusions within the ER that were found to be endoglycosidase H sensitive polymers (21,23). ΔNS neuroserpin displayed diffuse ER staining but no signal was detected within the Golgi complex (results not shown), suggesting that none of the misfolded mutant protein was trafficked out of the ER. We next quantified neuroserpin secretion from each cell line by metabolic labelling with ^{35}S-methionine/cysteine followed by immunoprecipitation of neuroserpin, SDS-PAGE and autoradiography. WT neuroserpin was almost completely secreted into the culture medium by 4 hours, compared with 78% and 18% of S52R and G392E neuroserpin respectively (Fig. 1b). ΔNS neuroserpin was not detected in the culture medium despite being cleared from the cell lysates within 1 hour of chase (Fig. 1b).

We predicted that ΔNS neuroserpin would be a substrate for ERAD. To test this hypothesis we investigated the degradation of each neuroserpin variant by pulse-chase in the presence or absence of lactacystin (which irreversibly inhibits the proteasome (25) or leupeptin (which inhibits lysosomal proteases (26,27). Treatment with lactacystin increased intracellular WT, S52R, G392E and ΔNS neuroserpin by 1.3, 1.6, 2.7 and 9.5-fold respectively (Fig. 1c, middle panels and graph). In contrast treatment with leupeptin had no effect on the intracellular levels of any neuroserpin species, suggesting lysosomal protease digestion plays a limited role in the degradation of mutant neuroserpin (Fig. 1c, bottom panels and graph).

Taken together, these data demonstrate that WT neuroserpin traffics normally through the secretory pathway and that S52R and G392E neuroserpin are secreted less efficiently and partially retained within the ER of PC12 cell lines. ΔNS neuroserpin is synthesized in the ER but rapidly cleared by ERAD without a detectable fraction being secreted into the media.

The accumulation of neuroserpin polymers within the ER does not activate the UPR

We next characterised the nature of the proteins retained within the ER up to 10 days after induction of expression by non-denaturing PAGE and Western Blot analysis of PC12 cell lysates (Fig. 2a). WT neuroserpin migrated as a single monomeric band whilst S52R and G392E neuroserpin formed the high molecular mass ladders that are characteristic of serpin polymers (Fig. 2a, native gel panels, arrow and bracket). A proportion of S52R neuroserpin migrated as a monomeric band (Fig. 2a, S52R, native, arrow). Although we could detect the presence of ΔNS neuroserpin by Western Blot after SDS-PAGE, we did not see any signal after non-denaturing PAGE, probably due to lower steady state levels of this mutant protein and/or the inability of this misfolded protein to be resolved by non-denaturing PAGE.

Since the mutants of neuroserpin accumulated within the ER, we next assessed their effect on the UPR. None of the proteins activated the UPR as assessed by expression levels of glucose regulated protein 94 (GRP94), immunoglobulin heavy chain binding protein (BiP) and protein disulphide isomerase (PDI) (Fig. 2a). In contrast, tunicamycin, a canonical UPR stimulus that inhibits N-linked glycosylation, caused an increase in the steady state levels of all these ER luminal chaperones (Fig. 2a, DMSO vs. Tun). Nuclear lysates were prepared from the same samples and analysed for the upregulation of C/EBP Homologous Protein (CHOP), a transcription factor specifically activated by the UPR (22,28). There was no detectable CHOP expression in any of the PC12 cell lines expressing neuroserpin (data not shown).

The apparent absence of a UPR even in response to ΔNS, the ERAD substrate, might represent an issue of sensitivity. We therefore assessed the activation of the UPR by the splicing of X-box binding protein 1 (*XBP1*) mRNA, which reports

activation of inositol requiring enzyme 1 (IRE1), a proximal UPR sensor in the ER membrane. When the PC12 cell lines were induced to express wildtype or mutant neuroserpin with 10 μg/ml doxycycline for 4 days, no *XBP1* mRNA splicing was detected (Fig. 2b, XBP1u). In contrast, cells treated with 2 μg/ml tunicamycin generated a faster migrating species corresponding to spliced *XBP1* mRNA (Fig. 2b, Tun, XBP1u and XBP1s). We did detect *XBP1* mRNA splicing in cells expressing ΔNS neuroserpin when the cells were treated with the proteasome inhibitor MG132 for 16 hours prior to harvesting (Fig. 2b, ΔNS +/+).

This raised the possibility that the methods we had used to detect UPR activation were insufficiently sensitive to detect subtle perturbations caused by the expression of mutant neuroserpin. To address this concern, we next assessed the activation of ATF6 using a highly sensitive reporter construct (pAT6(5×)-Luc, also known as the pUPRE-Luc, (29)). In these experiments, co-transfection with pRL-TK 24 hrs prior to cell collection reported transfection efficiency (Fig. 2c and d). Only PC12 cells expressing ΔNS activated ATF6 ($p<0.001$, ΔNS vs WT, 2-way ANOVA with Bonferroni post test; Fig. 2c). This upregulation was increased when the cells were treated with 100 nM MG132 for 16 hrs prior to harvesting, while the other neuroserpin variants failed to activate ATF6 after proteasome inhibition ($p<0.001$, ΔNS –MG132 vs ΔNS +MG132, 2-way ANOVA with Bonferroni post test; Fig. 2d).

These data show that the ER accumulation of neuroserpin polymers does not activate the UPR and that this failure is not due to defective UPR signalling, since an appropriate activation of ATF6 and XBP1 splicing response occurred during accumulation of ΔNS neuroserpin.

The ER accumulation of neuroserpin polymers activates NF-κB

It has been reported that the accumulation of Z α_1-antitrypsin in the ER of hepatocytes can activate NF-κB (11,12). We therefore asked whether the accumulation of polymeric neuroserpin could also activate this transcription factor. The stable PC12 Tet-On cell lines expressing neuroserpin variants were induced with 10 μg/ml doxycycline and subsequently co-transfected with the NF-κB reporter pELAM1-Luc and the transfection efficiency reporter pRL-TK (Fig. 3). We found low levels of NF-κB activation in cells expressing WT and ΔNS neuroserpin ($p<0.001$, WT and ΔNS vs PC12, 2-way ANOVA with Bonferroni post test; Fig. 3a). The expression of ER-retained S52R and G392E neuroserpin, however, resulted in much higher levels of NF-κB activation than WT ($p<0.001$, S52R and G392E vs WT, 2-way ANOVA with Bonferroni post test; Fig. 3a). There was no further increase in NF-κB activation following the addition of MG132 (Fig. 3b), suggesting that NF-κB activation does not report the accumulation of ERAD substrates. The addition of conditioned media from PC12 cells expressing S52R and G392E neuroserpin to parental PC12 cells for 10 days did not activate NF-κB.

NF-κB activation by neuroserpin polymers is independent of eIF2α phosphorylation

In addition to IRE1 and ATF6, UPR signalling occurs via the ER localised kinase PERK (30,31), which has previously been shown to activate NF-κB by the phosphorylation of eIF2α (17,32,33). We investigated whether polymers of neuroserpin could activate NF-κB independently of the PERK branch of the UPR by using $eIF2\alpha^{A/A}$ knock-in cells, in which mutation of serine 51 to alanine renders eIF2α unable to be phosphorylated by PERK (32). Both $eIF2\alpha^{S/S}$ and $eIF2\alpha^{A/A}$ murine embryonic fibroblasts (MEF) were treated with 1 μM thapsigargin for 30 min to confirm that only the $eIF2\alpha^{S/S}$ cells could phosphorylate serine 51 when the UPR is activated (Fig. 4a). The $eIF2\alpha^{S/S}$ and $eIF2\alpha^{A/A}$ MEF cells were next transduced with parental pBABE VSV-G pseudotyped retrovirus alone (ψ) or encoding WT, S52R, G392E or ΔNS neuroserpin. Stable pools of neuroserpin transgene-expressing cells were selected with puromycin and neuroserpin expression levels were assessed in all the cell pools by SDS-PAGE and Western Blot analysis. The steady state levels of all neuroserpin variants were similar in cell lysates and culture media for both $eIF2\alpha^{S/S}$ and $eIF2\alpha^{A/A}$ cells (Fig. 4b, Cells and Medium). As a control, TNF-α, which activates NFκB via

phosphorylation of IkB, activated the NF-κB reporter in both eIF2α$^{S/S}$ and eIF2α$^{A/A}$ MEF cells ($p<0.005$, both MEF lines untreated vs 8 hrs TNF-α, t-test, Fig 4c). In contrast, only the eIF2α$^{S/S}$ MEF cell line activated NF-κB in response to the UPR activating agent thapsigargin, confirming the role of eIF2α phosphorylation in UPR-induced NFκB activation but not in TNFα signalling ($p<0.005$, eIF2α$^{S/S}$ untreated vs 8 hrs thapsigargin, t-test; $P>0.05$ eIF2α$^{A/A}$ untreated vs 8 hrs thapsigargin, Fig. 4c). The stable pools of neuroserpin transgene-expressing cells were then co-transfected with the NF-κB and control luciferase reporters, and the relative levels of NF-κB activity were determined. The empty virus control cells and cells expressing WT neuroserpin did not activate the NF-κB reporter ($p>0.05$, t-test, Fig. 4d, ψ and WT). ΔNS neuroserpin expressing cells were able to activate NF-κB in the eIF2α$^{S/S}$ MEF cells but this signal was abrogated in eIF2α$^{A/A}$ cell lines ($p<0.001$, ψ vs ΔNS in eIF2α$^{S/S}$; $p>0.05$ in eIF2α$^{A/A}$ cells, t-test, Fig. 4d, ΔNS), suggesting that in this case NF-κB activation is mediated through the PERK limb of the UPR. In contrast, the S52R and G392E neuroserpin polymer forming cell lines were able to activate NF-κB in both eIF2α$^{S/S}$ and eIF2α$^{A/A}$ MEF cell lines (Fig. 4d, S52R and G392E).

These data provide clear evidence that the accumulation of ordered protein polymers within the ER can active NF-κB independently of the canonical UPR signalling pathway.

Polymer associated NF-κB activation is attenuated by sequestering intracellular calcium

Activation of NF-κB has previously been shown to be dependent on calcium (13,34,35). We therefore treated the PC12 cell lines induced to express neuroserpin with chelators of either extracellular (EGTA pH 7.4) or intracellular (BAPTA-AM) calcium. Increasing concentrations of EGTA had no effect on the activity of NF-κB in any of the cell lines (Fig. 5a). In contrast, chelating intracellular calcium resulted in a concentration-dependent reduction in NF-κB signalling in PC12 cells expressing WT, S52R, G392E and ΔNS neuroserpin (Fig. 5b). These agents induced only minimal cellular toxicity and had no effect on the ability of the mutants to form polymers (data not shown). To control for possible off-pathway toxic effects of the acetoxymethyl (AM) moiety liberated during the loading of cells with BAPTA-AM, we treated cells with another AM-ester, BCECF-AM, according to the manufacturer's instructions. We found that BCECF-AM, which does not chelate intracellular calcium, failed to affect activation of the NFκB reporter (data not shown). Cells expressing the polymer forming mutants of neuroserpin also showed a reduced ability to mobilise calcium when treated with 1 μM thapsigargin ($p<0.01$, PC12 vs G392E, 2-way ANOVA with Bonferroni post test; Fig. 5c), suggesting that polymer accumulation affects ER calcium homeostasis. A similar difference of intracellular calcium increase in response to thapsigargin was seen between WT and G392E neuroserpin-expressing cells when assayed in calcium-free OptiMEM medium (data not shown). This suggests that the effect of G392E neuroserpin is primarily on the release of ER calcium stores, rather than modifying store operated calcium influx from the extracellular space.

Taken together these data show that increased NF-κB activity in response to the accumulation of neuroserpin polymers within the ER is dependent on increased Ca^{2+} flux to the cytosol.

Discussion

The serpinopathies are unusual amongst the conformational diseases in that they result from the retention of ordered polymers, rather than unfolded proteins, within the ER of the cell of synthesis (1,2). This is most strikingly displayed in the dementia FENIB that is characterised by the intra-neuronal retention of polymers of neuroserpin as inclusions or Collin's bodies (5,6). We have assessed the effect of these intracellular inclusions in cell lines that conditionally express WT neuroserpin, mutants that cause moderate (S52R) and severe (G392E) forms of FENIB and a truncated misfolding version of neuroserpin that is a substrate for ERAD (ΔNS).

In our PC12 cell lines, WT neuroserpin was normally trafficked through the secretory pathway, as we have previously shown (23), whilst the truncated ΔNS neuroserpin was rapidly degraded

by ERAD with a half-life of approximately 30 min. This is similar to the cellular handling of the homologous Null Hong Kong variant of α_1-antitrypsin (24). The S52R and G392E mutants of neuroserpin that underlie FENIB (6) were retained as polymers within the ER as shown before (21). Intracellular levels of all neuroserpin mutants increased when cells were treated with the proteasome inhibitors lactacystin and MG132 (Fig. 1c and results not shown). This indicates that there is a soluble misfolding fraction of S52R and G392E mutant neuroserpin that can be degraded by ERAD (Fig. 7). In contrast, the inhibition of lysosomal degradation had little effect on the clearance of S52R and G392E neuroserpin. This suggests that autophagy may not be as important in the degradation of neuroserpin polymers in contrast to polymers of Z α_1-antitrypsin (36,37).

The retention of polymers of S52R and G392E neuroserpin within the ER had no effect on the expression levels of the UPR dependent ER chaperones GRP94, BiP or PDI (Fig. 2a). These chaperones were unaffected when intracellular concentrations of mutant proteins were increased by proteasome inhibition (results not shown). The expression of truncated ΔNS neuroserpin similarly had no effect, suggesting that the expression levels of these ER chaperones were insensitive to low level accumulation/misfolding of proteins within the ER. Truncated ΔNS neuroserpin was able, however, to elicit the splicing of *XBP1* mRNA when its intracellular levels were raised by proteasome inhibition, whereas polymers of mutant neuroserpin had no effect on *XBP1* mRNA splicing even when their levels were increased with the same treatment (Fig. 2b). This lack of UPR activation upon neuroserpin polymer accumulation was also apparent when characterised by a more sensitive assay, based on the pAT6(5x)-Luc or UPRE-driven luciferase reporter plasmid (Fig. 2c).

Although the accumulation of polymeric neuroserpin within the ER did not cause splicing of *XBP1* mRNA or activation of ATF6, it did activate NF-κB (Fig. 3). This activation of NF-κB was similar to that previously reported for cell and mouse models of α_1-antitrypsin deficiency (11,12). Previous work has shown that the activation of the UPR can induce NF-κB signalling through PERK (17,33). We therefore used mouse embryonic fibroblast (MEF) cells deficient in the PERK signalling branch of the UPR in order to assess polymer activation of NF-κB in more detail. Polymers of neuroserpin, but not the ERAD substrate ΔNS neuroserpin, were able to activate NF-κB in MEF eIF2α^{AA} cells (Fig. 4). These data confirm that neuroserpin polymers can activate NF-κB by a pathway that is independent of the canonical UPR (Fig. 6). This is reminiscent of an ER to nucleus signalling pathway that has been termed the EOR (13,14,38). The EOR was initially described in the context of adenovirus E3/19K protein and ΔF508 mutant of cystic fibrosis transmembrane conductance regulator (CFTR) accumulation, and has been proposed as the signalling pathway that operates upon accumulation of α_1-antitrypsin polymers within hepataocytes (11,12). Our results support the existence of a UPR-independent ER stress-signaling pathway that activates NF-κB. The term 'ER overload response' (13), however, may not be the most accurate to describe serpin polymer-mediated activation of NF-κB. This is because the overload of any protein that causes physical disruption of the ER would be associated with a reduction in ER efficiency and/or perturbance of Ca^{2+} homeostasis and the induction of ER stress (39,40). Furthermore, there were no morphological changes in the ER caused by polymer accumulation in our PC12 cell lines that would justify the term "overload" (data not shown). Moreover, the term EOR does not distinguish between misfolded proteins, such as CFTR (15) or correctly folded proteins, such as viral inclusions (14) or polymers of neuroserpin and α_1-antitypsin. We therefore suggest that 'ordered protein response' (OPR) would be a more appropriate name for this pathway to contrast with the unfolded protein response (UPR).

The EOR is associated with mobilisation of intracellular calcium (35,41-44). We therefore assessed the effect of extrinsic and intrinsic calcium chelators on the UPR (ΔNS neuroserpin) and OPR (polymer-mediated) activation of NF-κB. Extracellular chelation of calcium had little effect on either UPR or OPR-mediated activation of NF-κB. In contrast, signalling of NF-κB was attenuated by the chelation of intracellular Ca^{2+}. This was most striking for the cell lines expressing S52R and G392E neuroserpin. The intracellular capacity for calcium flux in the two polymer forming cell lines was significantly reduced when

Ca^{2+} was mobilised from the ER by the addition of 1 μM thapsigargin. These results suggest that ER Ca^{2+} regulation is involved in the polymer mediated activation of NF-κB in the OPR. Importantly neither secreted neuroserpin, nor extrinsic factors secreted by the neuroserpin cell lines into the culture medium, had any effect on the activity of NF-κB in parental PC12 cells. Thus, this cell-autonomous signal must derive from the site of intracellular polymer accumulation. Therefore, the activation of NF-κB by mutant polymer accumulation in PC12 cells is mediated by a calcium dependent process involved in transducing the signal from the ER to the nucleus.

In summary, we have dissected the signalling mediators that activate the transcription factor NF-κB following the accumulation of polymers of neuroserpin within the ER. This work supports the existence of an UPR independent ER-to-nucleus signal transduction pathway that corresponds to the EOR, but for accuracy, we propose to name it the "ordered protein response" or OPR. This pathway is also likely to be activated by the accumulation of ordered polymers of mutant α_1-antitypsin and in other serpinopathies. Transient activation of NF-κB in response to ER ordered polymers might regulate key pathways induced during cellular stress, such as proliferation, metabolic activity and differentiation (45). However, chronic activation of NF-κB may contribute to the cell death that underlies the accumulation of polymers of neuroserpin and α_1-antitypsin to cause dementia and cirrhosis respectively.

Acknowledgements

This work was supported by the Medical Research Council (UK) and Papworth NHS Trust. SJM is a MRC Clinician Scientist. RJK is an Investigator of the Howard Hughes Medical Institute and is supported by NIH grants RO1-DK042394, RO1-HL052173 and PO1-HL057346. We are grateful to Dr Timothy Weaver (Cincinnati Children's Hospital Medical Center, Cincinnati, Ohio, USA) for the pATF6(5×)-Luc, pELAM1-Luc and pRL-TK luciferase reporters. MJD wishes to thank all members of the Lomas lab and Dr. Karin Römisch for help and guidance.

References

1. Carrell, R. W., and Lomas, D. A. (1997) *Lancet* **350**, 134-138
2. Lomas, D. A., and Carrell, R. W. (2002) *Nat Rev Genet* **3**, 759-768
3. Gooptu, B., Hazes, B., Chang, W. S., Dafforn, T. R., Carrell, R. W., Read, R. J., and Lomas, D. A. (2000) *Proc Natl Acad Sci U S A* **97**, 67-72
4. Sivasothy, P., Dafforn, T. R., Gettins, P. G., and Lomas, D. A. (2000) *J Biol Chem* **275**, 33663-33668
5. Davis, R. L., Shrimpton, A. E., Holohan, P. D., Bradshaw, C., Feiglin, D., Collins, G. H., Sonderegger, P., Kinter, J., Becker, L. M., Lacbawan, F., Krasnewich, D., Muenke, M., Lawrence, D. A., Yerby, M. S., Shaw, C. M., Gooptu, B., Elliott, P. R., Finch, J. T., Carrell, R. W., and Lomas, D. A. (1999) *Nature* **401**, 376-379
6. Davis, R. L., Shrimpton, A. E., Carrell, R. W., Lomas, D. A., Gerhard, L., Baumann, B., Lawrence, D. A., Yepes, M., Kim, T. S., Ghetti, B., Piccardo, P., Takao, M., Lacbawan, F., Muenke, M., Sifers, R. N., Bradshaw, C. B., Kent, P. F., Collins, G. H., Larocca, D., and Holohan, P. D. (2002) *Lancet* **359**, 2242-2247
7. Davis, R. L., Holohan, P. D., Shrimpton, A. E., Tatum, A. H., Daucher, J., Collins, G. H., Todd, R., Bradshaw, C., Kent, P., Feiglin, D., Rosenbaum, A., Yerby, M. S., Shaw, C. M., Lacbawan, F., and Lawrence, D. A. (1999) *Am J Pathol* **155**, 1901-1913
8. Ron, D., and Walter, P. (2007) *Nat Rev Mol Cell Biol* **8**, 519-529
9. Marciniak, S. J., and Ron, D. (2006) *Physiol Rev* **86**, 1133-1149
10. Graham, K. S., Le, A., and Sifers, R. N. (1990) *J Biol Chem* **265**, 20463-20468
11. Hidvegi, T., Schmidt, B. Z., Hale, P., and Perlmutter, D. H. (2005) *J Biol Chem* **280**, 39002-39015
12. Lawless, M. W., Greene, C. M., Mulgrew, A., Taggart, C. C., O'Neill, S. J., and McElvaney, N. G. (2004) *J Immunol* **172**, 5722-5726
13. Pahl, H. L., and Baeuerle, P. A. (1995) *Embo J* **14**, 2580-2588
14. Pahl, H. L., Sester, M., Burgert, H. G., and Baeuerle, P. A. (1996) *J Cell Biol* **132**, 511-522
15. Knorre, A., Wagner, M., Schaefer, H. E., Colledge, W. H., and Pahl, H. L. (2002) *Biol Chem* **383**, 271-282
16. Pahl, H. L. (1999) *Physiol Rev* **79**, 683-701
17. Deng, J., Lu, P. D., Zhang, Y., Scheuner, D., Kaufman, R. J., Sonenberg, N., Harding, H. P., and Ron, D. (2004) *Mol Cell Biol* **24**, 10161-10168
18. Belorgey, D., Crowther, D. C., Mahadeva, R., and Lomas, D. A. (2002) *J Biol Chem* **277**, 17367-17373
19. Bartz, S. R., and Vodicka, M. A. (1997) *Methods* **12**, 337-342
20. Lu, P. D., Jousse, C., Marciniak, S. J., Zhang, Y., Novoa, I., Scheuner, D., Kaufman, R. J., Ron, D., and Harding, H. P. (2004) *Embo J* **23**, 169-179
21. Miranda, E., Romisch, K., and Lomas, D. A. (2004) *J Biol Chem* **279**, 28283-28291
22. Marciniak, S. J., Yun, C. Y., Oyadomari, S., Novoa, I., Zhang, Y., Jungreis, R., Nagata, K., Harding, H. P., and Ron, D. (2004) *Genes Dev* **18**, 3066-3077
23. Miranda, E., MacLeod, I., Davies, M. J., Perez, J., Romisch, K., Crowther, D. C., and Lomas, D. A. (2008) *Hum Mol Genet* **17**, 1527-1539
24. Sifers, R. N., Brashears-Macatee, S., Kidd, V. J., Muensch, H., and Woo, S. L. (1988) *J Biol Chem* **263**, 7330-7335
25. Fenteany, G., Standaert, R. F., Lane, W. S., Choi, S., Corey, E. J., and Schreiber, S. L. (1995) *Science* **268**, 726-731
26. Libby, P., and Goldberg, A. L. (1978) *Science* **199**, 534-536
27. Seglen, P. O. (1983) *Methods Enzymol* **96**, 737-764
28. Ma, Y., Brewer, J. W., Diehl, J. A., and Hendershot, L. M. (2002) *J Mol Biol* **318**, 1351-1365

29. Shen, J., and Prywes, R. (2005) *Methods* **35**, 382-389
30. Harding, H. P., Zhang, Y., and Ron, D. (1999) *Nature* **397**, 271-274
31. Harding, H. P., Zhang, Y., Bertolotti, A., Zeng, H., and Ron, D. (2000) *Mol Cell* **5**, 897-904
32. Scheuner, D., Song, B., McEwen, E., Liu, C., Laybutt, R., Gillespie, P., Saunders, T., Bonner-Weir, S., and Kaufman, R. J. (2001) *Mol Cell* **7**, 1165-1176
33. Jiang, H. Y., Wek, S. A., McGrath, B. C., Scheuner, D., Kaufman, R. J., Cavener, D. R., and Wek, R. C. (2003) *Mol Cell Biol* **23**, 5651-5663
34. Biswas, G., Anandatheerthavarada, H. K., Zaidi, M., and Avadhani, N. G. (2003) *J Cell Biol* **161**, 507-519
35. Lilienbaum, A., and Israel, A. (2003) *Mol Cell Biol* **23**, 2680-2698
36. Palmer, E. A., Kruse, K. B., Fewell, S. W., Buchanan, S. M., Brodsky, J. L., and McCracken, A. A. (2003) *J Cell Sci* **116**, 2361-2373
37. Teckman, J. H., and Perlmutter, D. H. (2000) *Am J Physiol Gastrointest Liver Physiol* **279**, G961-974
38. Pahl, H. L., and Baeuerle, P. A. (1997) *Trends Biochem Sci* **22**, 63-67
39. Michalak, M., Robert Parker, J. M., and Opas, M. (2002) *Cell Calcium* **32**, 269-278
40. Molinari, M., and Helenius, A. (2000) *Science* **288**, 331-333
41. Pahl, H. L., and Baeuerle, P. A. (1996) *FEBS Lett* **392**, 129-136
42. Kuang, E., Wan, Q., Li, X., Xu, H., Liu, Q., and Qi, Y. (2005) *J Cell Physiol* **204**, 549-559
43. Steffan, N. M., Bren, G. D., Frantz, B., Tocci, M. J., O'Neill, E. A., and Paya, C. V. (1995) *J Immunol* **155**, 4685-4691
44. Trushin, S. A., Pennington, K. N., Algeciras-Schimnich, A., and Paya, C. V. (1999) *J Biol Chem* **274**, 22923-22931
45. Perkins, N. D. (2007) *Nat Rev Mol Cell Biol* **8**, 49-62
46. Rock, K. L., Gramm, C., Rothstein, L., Clark, K., Stein, R., Dick, L., Hwang, D., and Goldberg, A. L. (1994) *Cell* **78**, 761-771

Figure Legends

Figure 1. Characterization of PC12 Tet-On cell lines expressing neuroserpin variants. (**A**) Schematic representation of neuroserpin variants used in this study. Full-length human neuroserpin is 410 amino acids long, with N-linked glycans at positions 157, 321 and 401, a signal peptide (32) and reactive centre loop (RCL) as indicated. The polymerogenic mutants have amino acid substitutions at positions 52 (S to R) and 392 (G to E) respectively and ΔNS has a premature stop codon at position 276. We generated PC12 Tet-On cell lines that stably expressed these constructs under the control of the tetracycline response element in the pTRE-Tight expression vector. (**B**) Secretion of neuroserpin variants. PC12 cells expressing WT, S52R, G392E and ΔNS neuroserpin were metabolically labelled with ^{35}S-met/cys for 15 min and chased for the times indicated. Neuroserpin was immunoprecipitated from cell lysates and culture medium, resolved by 10% w/v SDS-PAGE and quantified by autoradiography using a phosphorimager. The graph shows average +/- SD for three independent repeats. **(C)**. Intracellular degradation of neuroserpin variants. PC12 cells treated with DMSO (vehicle), 25 μM lactacystin (irreversible inhibitor of the proteasome) or 200 μM leupeptin (inhibitor of lysosomal proteases) were metabolically labelled and analysed as described in (B). The histograms show the amount of radiolabelled neuroserpin remaining after the chase normalized to the initial amount of neuroserpin for each condition, and values are averages +/- SEM of three independent repeats. Control experiments in PC12 cells with leupeptin and lactacystin showed the efficacy of the inhibitor treatments in blocking processing of pro-cathepsin D to mature cathepsin D and the degradation of cyclin B1 respectively (data not shown).

Figure 2. Accumulation of neuroserpin polymers within the ER does not activate the UPR. (A) Polymers of neuroserpin do not upregulate ER luminal chaperones. Neuroserpin expression was induced in PC12 cells with 10 μg/ml doxycycline for 10 days and cell lysates were resolved by 10% w/v SDS- and 7.5% w/v/ non-denaturing PAGE. Western Blot analysis for neuroserpin of SDS-PAGE (NS, SDS) revealed a 50 kDa band in WT, S52R and G392E neuroserpin expressing cells and 28 kDa in ΔNS neuroserpin cells. On non-denaturing PAGE (NS, native), WT neuroserpin migrated as a single monomer band (arrow), whereas S52R and G392E neuroserpin formed high molecular mass ladders that are characteristic of polymers (bracket). There was no detectable signal for ΔNS on non-denaturing PAGE. The expression levels of ER luminal chaperones regulated by the UPR [glucose regulated protein 94 (Grp94), immunoglobin heavy chain-binding protein (BiP) and protein disulphide isomerase (PDI)] were determined in the same membranes by Western Blotting. Treatment with 2 μg/ml tunicamycin (Tun) for 16 hr compared with vehicle alone (DMSO) was used as a positive control for UPR induction, and protein loading was assessed by Western Blot analysis for GAPDH. (**B**) Polymers of neuroserpin do not activate IRE1. The expression of WT, S52R, G392E and ΔNS neuroserpin was induced for 4 days with 10 μg/ml doxycycline (Dox) and cells were either harvested or treated 16 hr prior to RNA isolation with 100 nM MG132, a reversible inhibitor of the proteasome (46). XBP1 mRNA was amplified by PCR and resolved by 2% w/v TBE agarose gel electrophoresis. Unspliced XBP1 (XBP1u) and spliced XBP1 (XBP1s) products migrated at 486 and 457 bp respectively. Neuroserpin (NS) and β-actin cDNAs were amplified to demonstrate transgene induction and as loading controls, respectively. PC12 cells treated with 2 μg/ml tunicamycin (Tun) were used as a positive control for UPR induced XBP1 mRNA splicing. (**C**) and **(D)** Polymers of neuroserpin do not activate ATF6. Neuroserpin expression was induced in PC12 cell lines with 10 μg/ml doxycycline for 10 days. Twenty-four hrs prior to lysis the cells were co-transfected with a plasmid encoding firefly luciferase under the control of a UPR response element (p5×ATF6-Luc) and with the transfection efficiency reporter pRL-TK renilla luciferase. The graphs show firefly luciferase normalized to renilla luciferase as averages +/- SD of three repeats and values are expressed in relative light units (RLU). Cells were mock-treated (**C**) or treated with 100 nM MG132 (**D**) for 16 hrs prior to harvesting.

Figure 3. The ER accumulation of neuroserpin polymers activates NF-κB. Neuroserpin expression was induced in PC12 cell lines with 10 μg/ml doxycycline and cells harvested at 2 day intervals for up to 10 days. Twenty-four hrs prior to collection cells were co-transfected with a plasmid encoding a NF-κB driven luciferase reporter (pELAM1-Luc) and with the transfection efficiency reporter pRL-TK renilla luciferase. The graphs show firefly luciferase normalized to renilla luciferase as averages +/- SD of three repeats and values are expressed in relative light units (RLU). NF-κB was measured in cells mock-treated (**A**) or treated with 100 nM MG132 (**B**) for 16 hrs prior to harvesting.

Figure 4. Neuroserpin polymers expressed in eIF2α $S51^{A/A}$ MEF cells can still activate NF-κB. Wild type eIF2α $S51^{S/S}$ and PERK signalling deficient eIF2α $S51^{A/A}$ MEF cells were transduced with pBABE retrovirus alone (ψ) or encoding WT, S52R, G392E or ΔNS neuroserpin. (**A**) Only wild type eIF2α $S51^{S/S}$ cells can phosphorylate eIF2α. eIF2α $S51^{S/S}$ and eIF2α $S51^{A/A}$ MEF cells were treated as indicated with 1 μM thapsigargin (TG) for 30 min and allowed to recover for 3 hrs in fresh medium. Cell lysates were resolved by 10% w/v SDS-PAGE and phosphorylated-eIF2α detected by Western Blot analysis. GAPDH was used as a protein loading control. (**B**) Neuroserpin is similarly expressed and handled in eIF2α $S51^{S/S}$ and eIF2α $S51^{A/A}$ MEF cells. Cell lysates and culture media from puromycin selected stable pools of MEF cells expressing neuroserpin variants were resolved by 10% w/v SDS or 7.5% w/v non-denaturing PAGE (native), followed by Western Blot analysis for neuroserpin or GAPDH as a protein loading control. (**C**) eIF2α $S51^{A/A}$ MEF cells fail to activate NF-κB upon UPR induction with thapsigargin. eIF2α $S51^{S/S}$ and eIF2α $S51^{A/A}$ MEF cells were co-transfected with the NF-κB (pELAM1-Luc) and pRL-TK reporter plasmids as described in Fig.3. Cells were either treated with 1 μM thapsigargin (TG) for 30 min with recovery in fresh medium or 200 ng/ml TNF-α for the indicated times prior to lysis and luciferase assay. The graph shows firefly luciferase normalized to renilla luciferase as averages +/- SD of three repeats and values are expressed in relative light units (RLU). (**D**) eIF2α $S51^{A/A}$ MEF cells expressing polymer forming mutants of neuroserpin can activate NF-κB. eIF2α $S51^{S/S}$ and eIF2α $S51^{A/A}$ cells expressing WT or mutant neuroserpin were co-transfected with the NF-κB (pELAM1-Luc) and pRL-TK reporter plasmids as described in Fig.3, and the normalised activity of NF-κB expressed in RLU. The data are averages +/- SD of six independent experiments.

Figure 5. The activation of NF-κB by neuroserpin polymers depends on intracellular Ca^{2+}. Neuroserpin expression in PC12 cells was induced for 5 days with 10 μg/ml doxycycline, cells were co-transfected with NF-κB (pELAM1-Luc) and pRL-TK reporter plasmids as described in Fig.3 and the normalised activity of NF-κB expressed in RLU. The culture medium was supplemented 16 hrs prior to harvesting with increasing concentrations of (**A**) EGTA pH 7.4, a membrane-impermeable extracellular Ca^{2+} chelator or (**B**) BAPTA-AM, a membrane-permeable intracellular Ca^{2+} chelator. The values are averages +/- SD of three independent repeats. (**C**) Expression of neuroserpin in PC12 cell lines was induced for 5 days with 10 μg/ml doxycycline, or PC12 cells were treated with either 2 μg/ml tunicamycin (Tun) for 16 hrs or 1 μM thapsigargin (TG) for 30 min. All cells were subsequently loaded with Fluo-4 (Molecular Probes, Invitrogen, UK). Intracellular Ca^{2+} mobilisation was measured with an emission OD 488 nm over time with the addition of 1 μM thapsigargin (arrow), which induces Ca^{2+} efflux into the cytoplasm and excites the Fluo-4 chromophore. The data were collected using a FACScalibur (BD Biosceinces) flow cytometer and analysed with FlowJo; representative dataset of three independent repeats.

Figure 6. Molecular mechanism of NF-κB activation by serpin polymers. Newly synthesised serpin molecules enter the ER by co-translational translocation. Correctly folded molecules (native protein) are packaged into ER-to-Golgi transport vesicles for secretion (not shown), whereas folding intermediates and misfolded species are retained in the ER, where they can be targeted into the ERAD pathway. Some mutant serpins monomers (M) form homogenous ordered polymers (P) via partial RCL insertion

intermediates (M*), which escape the ER quality control system and form inclusion bodies. These inclusion bodies are in effect 'insoluble' to the cell, and may no longer be seen by the canonical quality control systems. Accumulated polymers of mutant serpins can elicit the specific activation of the transcription factor NF-κB independently of the UPR by increasing cytosolic Ca^{2+}.

Supplementary Figure 1. Dose-response for the induction of neuroserpin expression with doxycycline in PC12 Tet-On cell lines. PC12 cell lines were induced for 3 days with 0-10 μg/ml of doxycycline. Cell lysates were resolved by 10% w/v SDS-PAGE and analysed by Western Blot for neuroserpin and GAPDH as a protein loading control. Twenty nanograms of recombinant purified neuroserpin were loaded as a positive control.

Fig 1

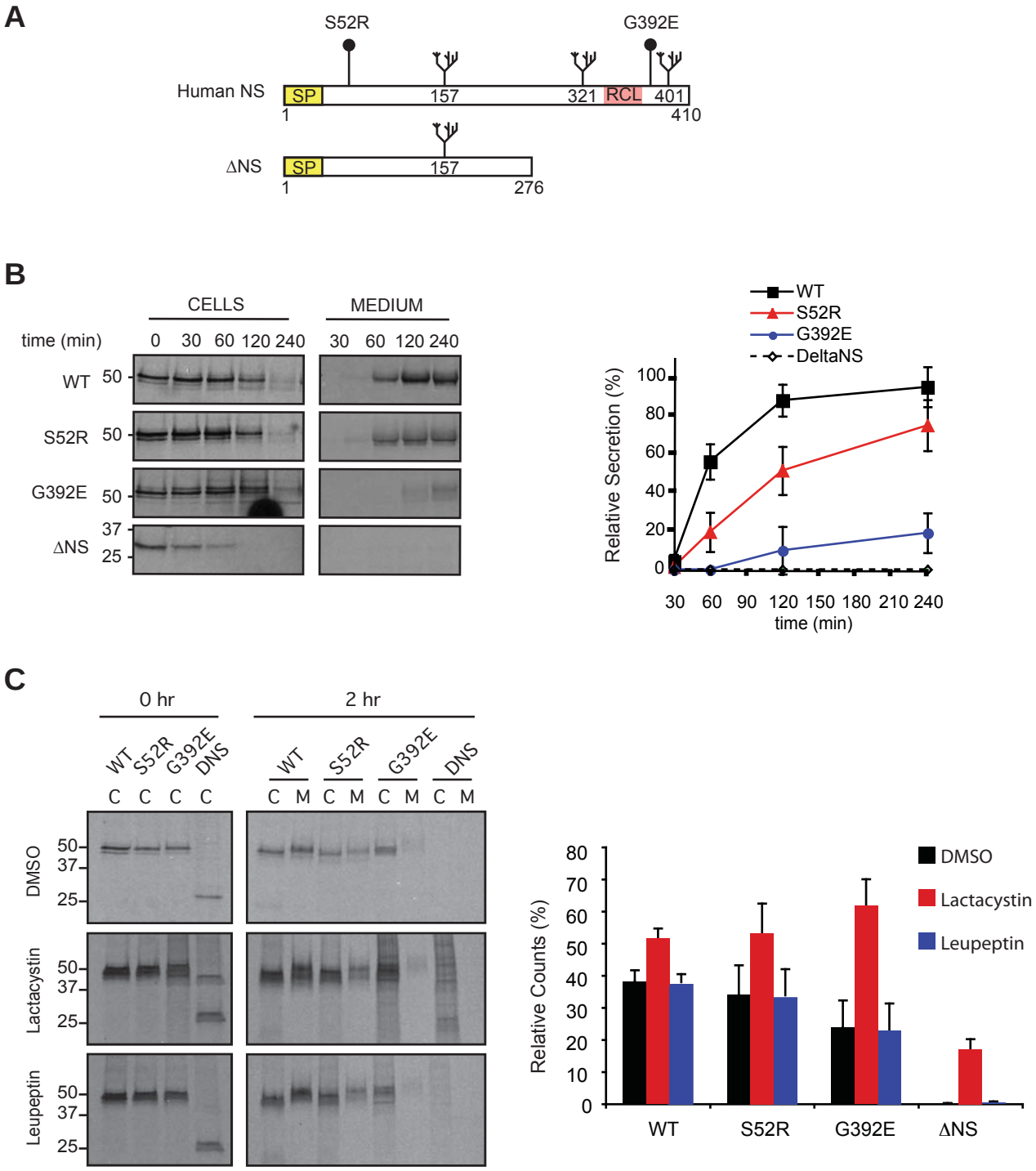
A
S52R
G392E
Human NS
SP
157
321
RCL
401
1
410
ΔNS
SP
157
1
276
B
CELLS
MEDIUM
time (min)
0 30 60 120 240
30 60 120 240
WT
S52R
G392E
ΔNS
50
50
50
37
25
WT
S52R
G392E
DeltaNS
Relative Secretion (%)
100
80
60
40
20
0
30 60 90 120 150 180 210 240
time (min)
C
0 hr
2 hr
WT
S52R
G392E
DNS
C C C C
C M C M C M C M
DMSO
Lactacystin
Leupeptin
50
37
25
Relative Counts (%)
80
70
60
50
40
30
20
10
0
DMSO
Lactacystin
Leupeptin
WT
S52R
G392E
ΔNS

Fig 2

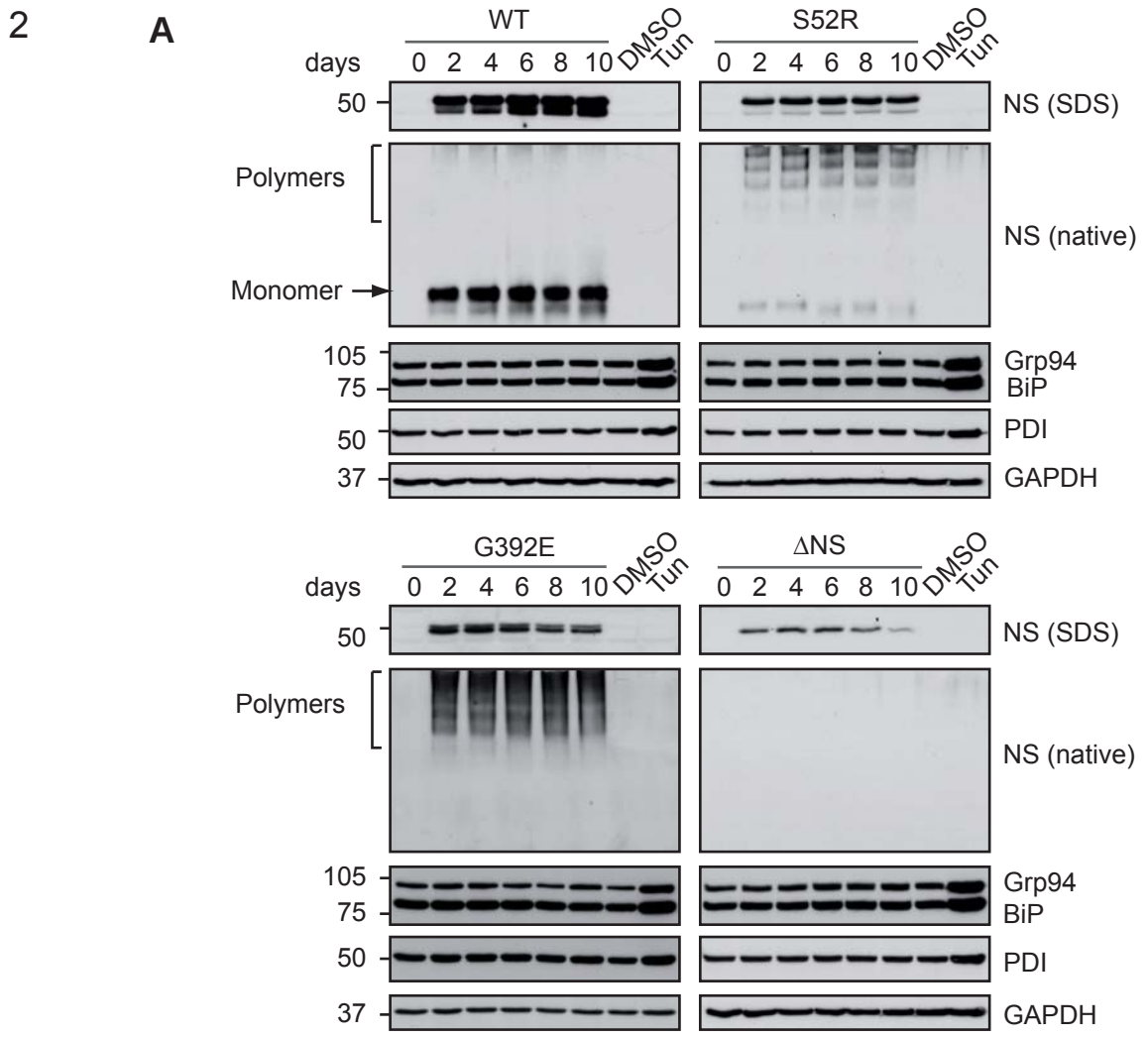
A
WT
S52R
G392E
ΔNS
days
0 2 4 6 8 10
DMSO
Tun
50
Polymers
Monomer
NS (SDS)
NS (native)
105
75
50
37
Grp94
BiP
PDI
GAPDH

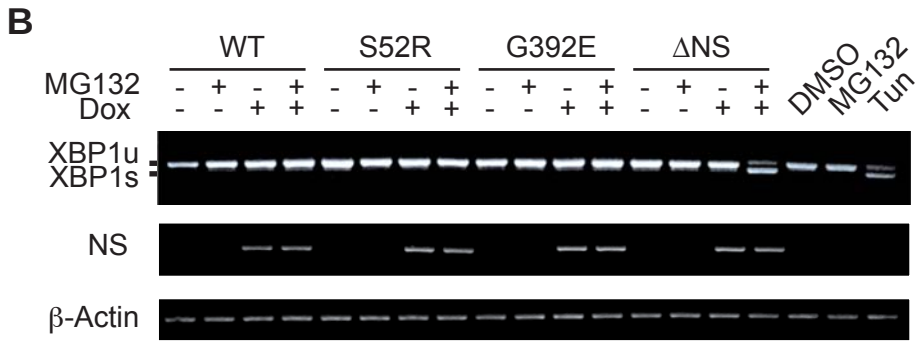
B
WT
S52R
G392E
ΔNS
MG132
Dox
DMSO
MG132
Tun
XBP1u
XBP1s
NS
β-Actin

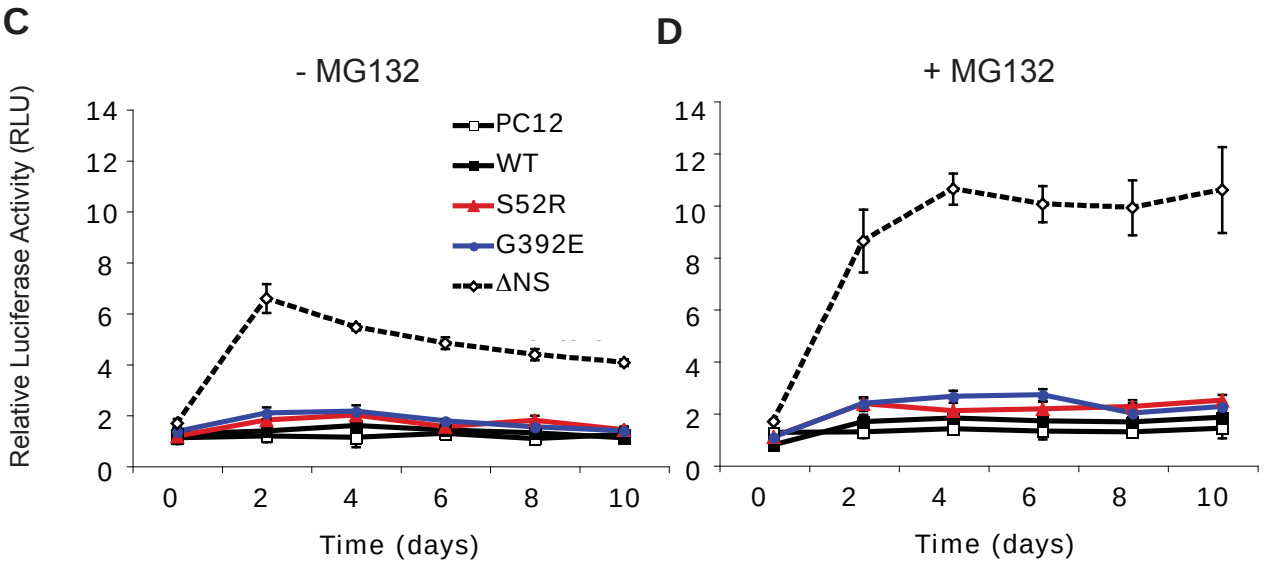
C
- MG132
D
+ MG132
Relative Luciferase Activity (RLU)
PC12
WT
S52R
G392E
ΔNS
0 2 4 6 8 10 12 14
0 2 4 6 8 10
Time (days)

Fig 3

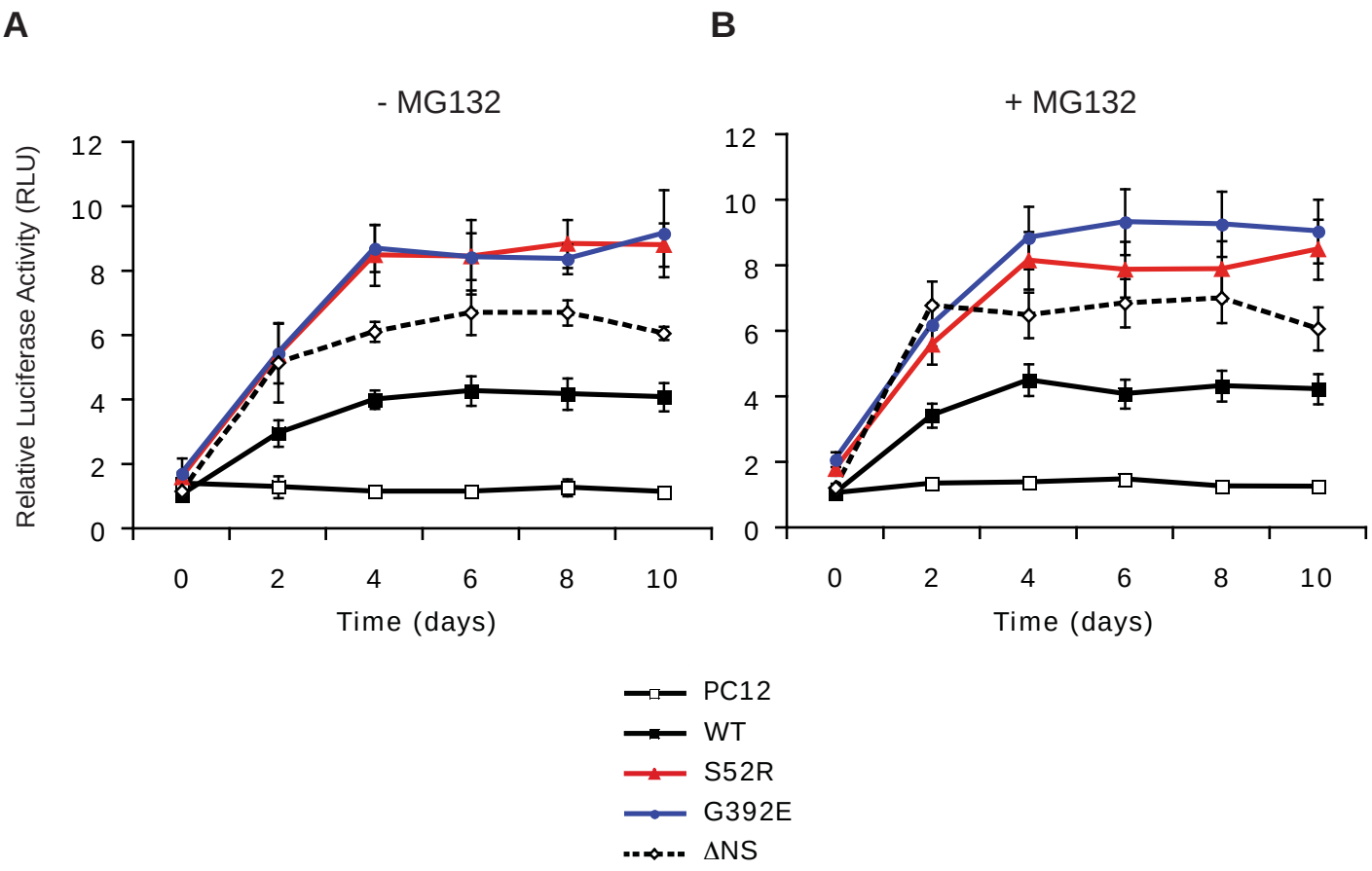
A
B
- MG132
+ MG132
Relative Luciferase Activity (RLU)
0
2
4
6
8
10
12
Time (days)
PC12
WT
S52R
G392E
ΔNS

Fig 4

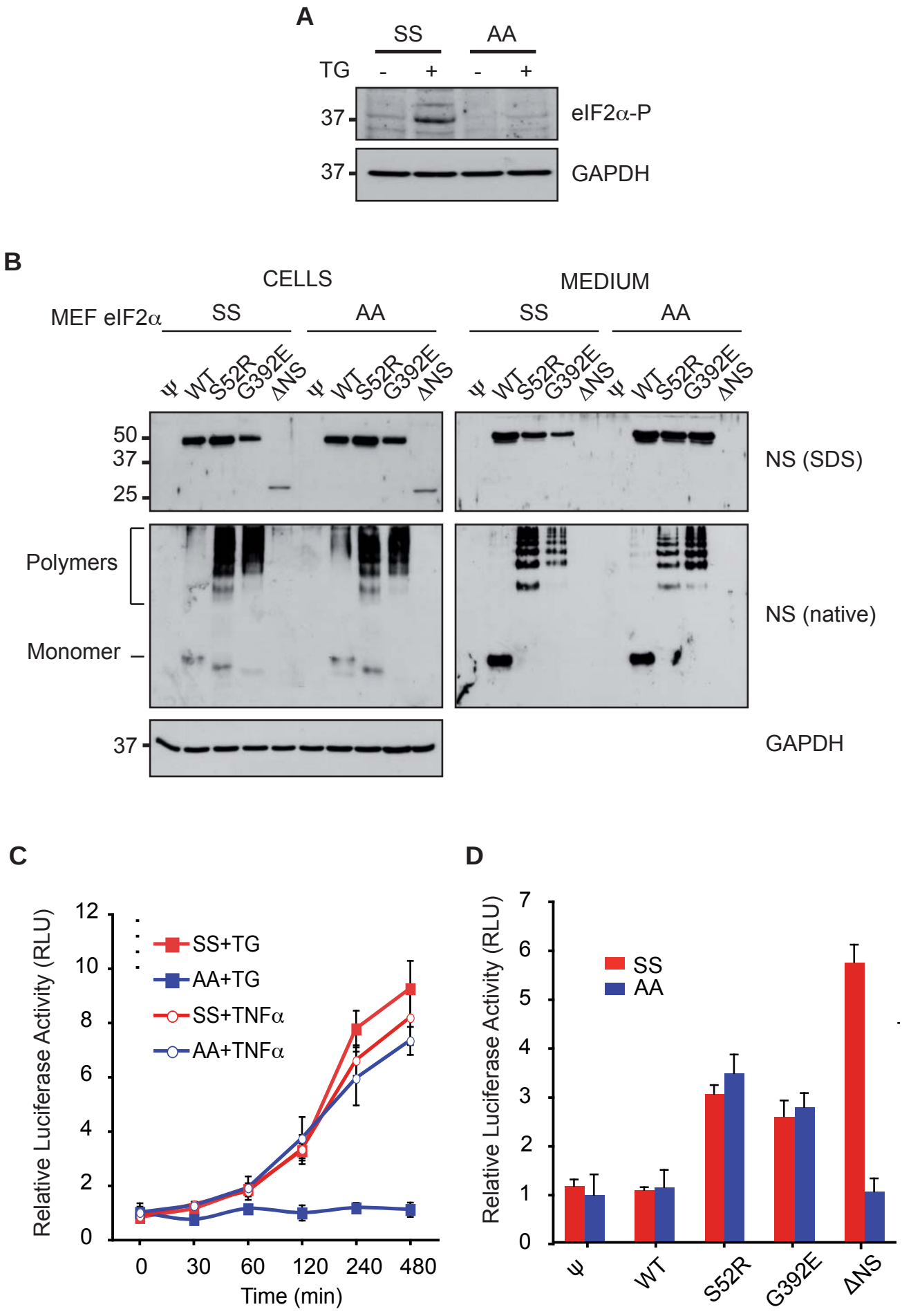
A
SS
AA
TG
-
+
-
+
37
eIF2α-P
37
GAPDH
B
CELLS
MEDIUM
MEF eIF2α
SS
AA
SS
AA
Ψ
WT
S52R
G392E
ΔNS
50
37
25
NS (SDS)
Polymers
Monomer
NS (native)
37
GAPDH
C
Relative Luciferase Activity (RLU)
12
10
8
6
4
2
0
SS+TG
AA+TG
SS+TNFα
AA+TNFα
0
30
60
120
240
480
Time (min)
D
Relative Luciferase Activity (RLU)
7
6
5
4
3
2
1
0
SS
AA
Ψ
WT
S52R
G392E
ΔNS

Fig 5

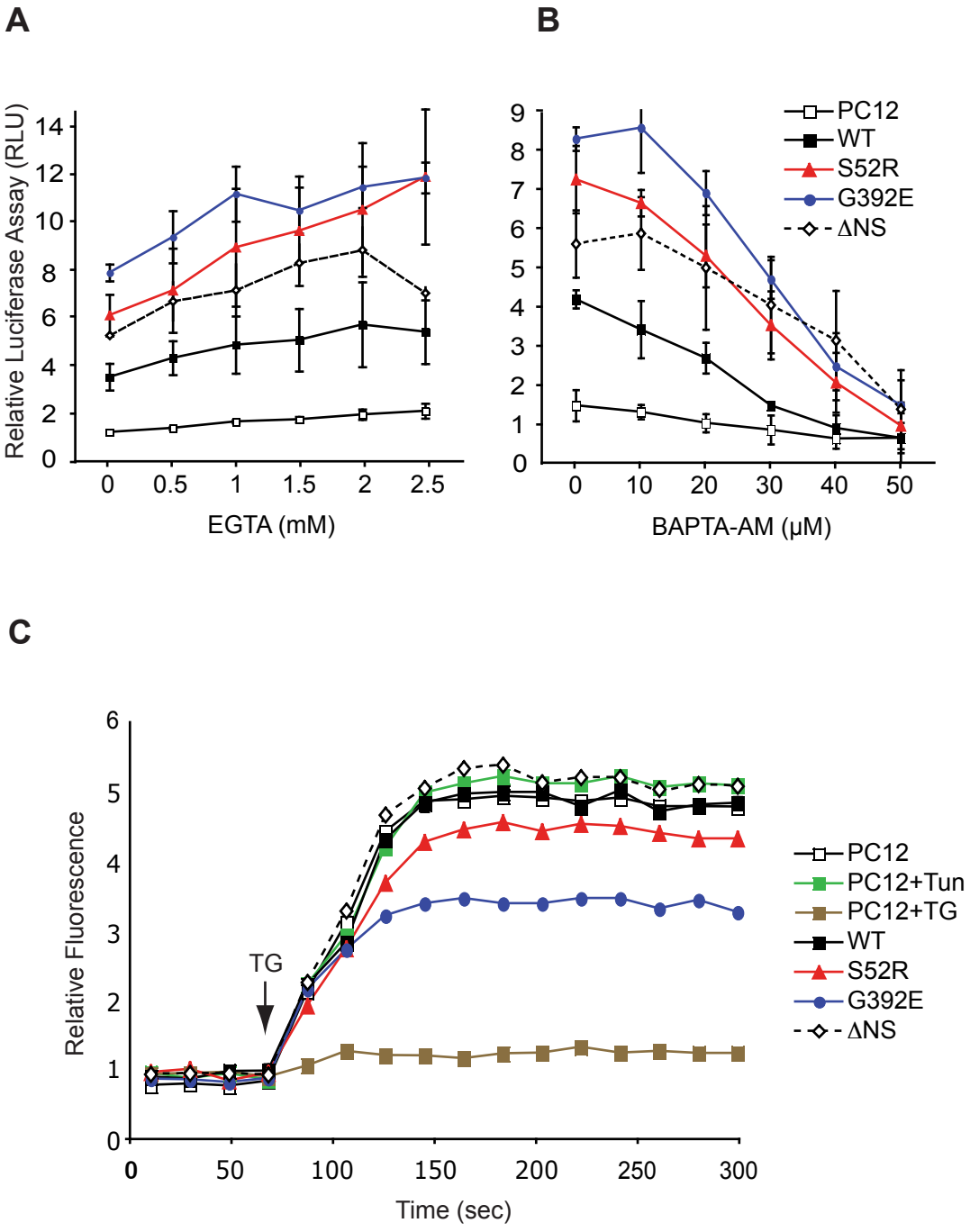
A
B
C
Relative Luciferase Assay (RLU)
EGTA (mM)
BAPTA-AM (μM)
PC12
WT
S52R
G392E
ΔNS
Relative Fluorescence
TG
Time (sec)
PC12
PC12+Tun
PC12+TG
WT
S52R
G392E
ΔNS

Fig 6.9

Fig 6

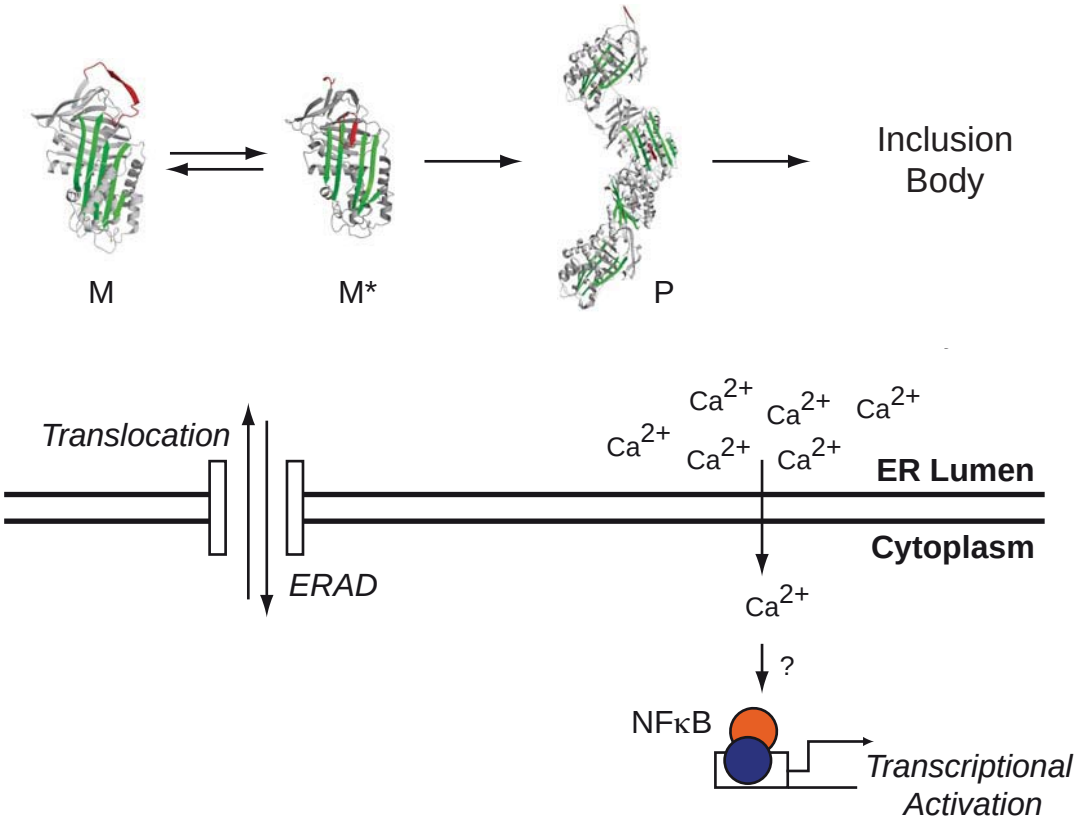
Inclusion Body
M
M*
P
Translocation
ERAD
Ca2+
Ca2+
Ca2+
Ca2+
Ca2+
Ca2+
ER Lumen
Cytoplasm
Ca2+
?
NFκB
Transcriptional Activation

Sup Fig 1